UltraViolet Index

by

Craig S. Long and Alvin J. Miller
Climate Prediction Center

Hai-Tien Lee and Jeannette D. Wild
Research and Data Systems, Inc.

Introduction

With the successful completion of the Experimental Ultraviolet Index program initiated June 28, 1994, the National Weather Service (NWS) in collaboration with the Environmental Protection Agency (EPA) began issuing the UltraViolet (UV) Index forecast as of April 3, 1995. The UV Index (UVI) is a mechanism by which the American public is forewarned of tomorrow's noontime intensity of UV radiation at locations within the U.S. The EPA's role in this effort is to alert the public of the dangerous health effects of overexposure to, and the accumulative effects of, UV radiation, as well as to provide ground level monitoring data for use in ongoing verification of the UVI. The National Weather Service calculates the UVI using existing atmospheric measurements, forecasts, and an advanced radiative transfer model. This paper will discuss the justification for a forecasted index, the nature of UV radiation, the methodology of producing the UVI, results from verifying the UVI, how the UVI is disseminated, and how to use the UVI information.

The Problem

Since World War II changes in the public's lifestyle have resulted in an increase in exposure (and overexposure) to UV radiation over a period of years to decades. This has contributed to an increase in the number of diagnoses of melanoma (i.e. skin cancer) and the number of cataract diagnoses has risen

melanoma skin cancers. This number of 9,200 deaths translates to greater than ***one death per hour*** in the U.S. Cataracts have been determined to cause 53% of the blindness cases worldwide. In addition, studies by DeFabo and Noonan, (1983) show that overexposure to the sun can suppress of the immune system. In response to these health related concerns, several countries have initiated public outreach campaigns to inform the public of the dangers of overexposure to the sun. These campaigns explain that simple remedial steps can be taken to greatly reduce the risk of overexposure, and are reinforced by the daily issuance of an index which informs the public of the potential intensity of the sun's UV radiation.

Brief History

Queensland, Australia started the first education campaigns on prevention of skin cancer and the hazards of overexposure to UV radiation. In the mid 1980's, the Australian Radiation Laboratory began monitoring UV radiation and broadcasting the day's UV dosage in minimum erythemal dosage units (MEDs) for all the states' capital cities during the evening news. Also, in 1987 New Zealand initiated public awareness campaigns along with the issuance of "burn time" reports broadcasted hourly on the radio. In 1992 the Atmospheric and Environment Service (AES) of Canada began issuing their own UV Index (Wilson, 1993), a next day forecast of UV exposure on a scale of 0 - 10 (where 10 is the highest value likely in southern Canada). All three countries have had very good success in getting the message to the public about the dangers of being in the sun too long and the possible consequences to the skin, eyes and immune system over a prolonged period of time (Decima Research, 1993, Hill et al., 1993, Colmar Brunton Research, 1992).

In 1993 the Environmental Protection Agency (EPA) approached the National Weather Service (NWS) to develop and generate an

number of treatments for skin cancer and cataract surgery could lead to savings in the billions of dollars in health care. Prevent Blindness America, a group advocating preventative measures, cites from existing data up to 1993 that there are about 1.35 million cataract surgeries performed annually in the U.S. This costs the taxpayers $3.4 billion in Medicare costs. It is unknown what fraction of these cataract cases are directly attributable to overexposure to UV radiation, but the emphasis is that there is a great potential for reducing costs by very simple measures like wearing broad rimmed hats and protective sunglasses.

On June 28, 1994 the National Weather Service initiated this program on an experimental basis for a limited number of sites. The Experimental UV Index consisted of a forecast of the next day's noon hour's UV intensity with adjustments for clouds and elevation. This forecast was made available for 58 cities within the contiguous U.S., Alaska, Hawaii, and Puerto Rico. The time following the launch of this product was used to test for any difficulties in the dissemination of the UVI, to conduct studies to see if the centrally produced forecast could be improved upon at the local level , to gain experience with respect to public perception of the UVI, and most importantly to check the validity of the forecasts. With the successful completion of this experimental phase, authority was given to expand the scope of the UVI and make it a fully operational product. It should be noted that UVI forecasts for Hawaii and Puerto Rico do not include any cloud attenuation due to the absence of MOS cloud probabilities for these locations.

Nature of UV Radiation

UV radiation can be divided into three parts of the sun's radiation spectrum. UV-C is characterized by wavelengths less than 280 nm. Although highly dangerous to plants and animals

cataracts and suppression of the immune system in the long term. The wavelengths of UV-A range between 320 and 400 nm. Ozone absorbs very little of this part of the UV spectrum. UV-A radiation is needed by humans for the synthesis of vitamin-D; however, too much UV-A causes photoaging (toughening of the skin), suppression of the immune system and to a lesser degree reddening of the skin and cataract formation.

The intensity of UV radiation reaching the surface under clear sky conditions is dependent upon the angle of incidence of the sun's rays to the earth's surface, the closeness of the sun to the Earth, and the amount of ozone in the atmosphere. This means that UV radiation increases from the polar regions, were the sun is very low in the sky, to the tropics where it lies overhead. Seasonally and daily, as the sun's elevation in the sky changes, so does the amount of UV radiation. Figure 1 shows how the UV radiation levels are minimal in the early morning and late evening and are greatest at mid-day, when the sun is highest in the sky. The NWS forcasts the UVI for the time of day when the sun is highest in the sky. However, the presence of clouds or other absorbing/scattering media may attenuate the amount of UV radiation reaching the surface.

Operational Procedure

The UV radiation at the surface is derived using a radiative transfer model (Frederick and Lubin, 1988). This model requires a few inputs to compute a "clear sky" (no clouds) determination of the irradiances throughout the UV spectrum. These inputs include: the total column ozone above the location of interest, the location's latitude, the day of year and the time of the solar day. The model uses the latter three inputs to determine the sun-earth distance, hence the amount of solar radiation reaching the top of the atmosphere, and the solar zenith angle. The solar zenith angle determines both the angle of incidence of the UV radiation at the earth's surface, and the distance the UV radiation travels through the atmosphere. As the path length becomes greater so does the absorption and scattering of UV

of day, and the amount and thickness of clouds overhead. Other factors that either enhance or attenuate the UV intensity are elevation, surface albedo, tropospheric pollution and haze. UV radiation does increase with increasing altitude. It also can be reflected by water, sand, concrete and snow by significant amounts (Blumthaler and Ambach, 1988, Coulson and Reynolds, 1971, and Kondratyev, 1969).

The NWS obtains ozone amounts from polar orbiting satellites and determines cloud amounts from its numerical models. A site's elevation is looked up from a gridded elevation field knowing its latitude and longitude. Currently, the UVI holds the surface UV albedo constant at 5%, and uses an optical depth of 0.2. The effects and the forecast of tropospheric pollution and haze on UV radiation still require more research and are not included in the current UVI.

Sources of Ozone Data

Ozone information needed to determine the UV radiation at the surface is available to the NWS from several sources. Two instruments on board a number of different satellites currently detect total column ozone. The Solar Backscattering UltraViolet Ozone Sensor/2 (SBUV/2) instrument obtains a vertical profile of ozone within a nadir viewed footprint. This instrument resides on board the currently operating NOAA-14 satellite as well as the previously operating NOAA-11 and NOAA-9 satellites. Full global coverage of the sunlit portion of the earth is achieved from each as the satellite orbits the earth 14 times per day. The data from this instrument is processed in a routine mode at NOAA. Because of the small geographical coverage of the nadir viewed total column ozone data footprints, a Cressman-adjustment scheme is used to incorporate the observed data into an existing gridded analysis of the hemispheric ozone data (Nagatani et al., 1977). A second instrument, the TIROS Operational Vertical Sounder (TOVS), provides another source of total column ozone. This instrument is also on board previous NOAA satellites as well as the current NOAA-14 satellite. The TOVS instrument provides horizontally resolved data and is also available as an

SBUV/2 data becomes unavailable.

Forecasting the Ozone Field

The routinely processed total column ozone data obtained from the SBUV/2 instrument exist as two hemispheric 65x65 polar grids. The UVI processor translates these fields to a 1"x 1" or 181x360 point equal latitude/longitude grid. This is done to ensure equal weighting of all latitudes. This ozone field is for "yesterday", and a forecast of "tomorrow's" ozone field must be made in order to create a forecast of "tomorrow's" UV levels. It has been shown that the total column ozone field correlates positively with the 50 hPa temperature field (T_{50}) (eg. Miller et al., 1979) and, to a lesser degree, negatively with the 100 and 500 hPa geopotential height fields (Z_{100} and Z_{500}, respectively). We assume that the relationship of changes in the ozone field to changes in the height and temperature fields from "two days ago" to "yesterday" will be applicable to determine the changes of the ozone field from "yesterday" to "tomorrow". Two sets of differences are needed to carry out this procedure. The first set is made up of the differences between "yesterday" and "two days ago". These are computed for the ozone, temperature and height fields. A separate regression for the Northern and Southern Hemisphere between the ozone differences and the height, and temperature differences is computed. This is done to preserve the seasonal differences between the two hemispheres. The second set of differences is determined from the MRF's forecast fields for "tomorrow" and the analysis fields from "yesterday". Using the regression coefficients and the second set of differences we "predict" the ozone difference field between "yesterday" and "tomorrow". Equation 1 summarizes the above narrative, where:

$\triangle O_3$ is the predicted change in total column ozone from "yesterday" to "tomorrow",

$\triangle Z_{100}$ and $\triangle Z_{500}$ are the changes in geopotential height at 100 and 500 hPa from "yesterday" to "tomorrow", respectively,

$\triangle T_{50}$ is the changes in temperature at 50 hPa from "yesterday" to "tomorrow",

a, b and c are regression coefficients and d is the

$$a \approx \frac{\delta O_3}{\delta Z_{500}} \quad , \quad b \approx \frac{\delta O_3}{\delta Z_{100}} \quad , \quad c \approx \frac{\delta O_3}{\delta T_{50}} \qquad (2),$$

where $\delta O_3/\delta X$ is the change in ozone with respect to the heights and temperature fields for "two days ago" to "yesterday". The "predicted" ozone differences are added to "yesterday's" ozone field producing a "predicted" ozone field for "tomorrow" as shown in Equation 3. This procedure, including the generation of new regression coefficients, is performed each day.

$$O_3(tomorrow) = O_3(yesterday) + \Delta O_3 \qquad (3)$$

The above approach, as opposed to a direct ozone -to-meteorological parameter regression, preserves the maximum and minimum values of ozone whcih have the greatest impact on surface UV radiation.

Figure 2 shows the scatter plots for the forecast Northern Hemisphere(NH) ozone field vs the observed NH ozone field for dates near the equinoxes and solstices. The March date shows the largest dynamic range of ozone values, and the September date shows the smallest. In general, the high ozone values occur at high latitudes, and the low ozone values occur in the tropics. Table 1 shows that the correlation coefficients(r) for the March and June dates (.97 and .94, respectively) are highest while September and December (.43 and .49, respectively) are the lowest. Large correlation coefficients, however, can be achieved by having a large dynamic range. The mean difference (forecast-analysis) and the RMS error may be a better indicator of the quality of the ozone forecast. The mean difference for March is 0.01 DU, but its RMS error is 14.7 DU. The mean differences (0.53 and 0.53 DU) and RMS errors (9.3 and 9.9 DU) for June and September are about the same. December has a negative mean difference (-0.43 DU) and a RMS error of 11.3 DU. The forecast

Jun. 23, 1992	0.94	0.53	9.3
Sep. 23, 1992	0.43	0.53	9.3
Dec. 23, 1992	0.49	-0.43	11.3

Table 1. Resulting statistics of comparisons of forecasts and observations for four NH seasons.

Is all the above work to produce a forecast of ozone better than using persistence(i.e. using "yesterday's" ozone field as "tomorrow's")? Table 2 illustrates that for the NH the RMS forecast error during the period from December 24, 1993 to February 5, 1994 is lower than using persistence for a 2 ("yesterday" to "tomorrow") through 5 day forecast. The forecast and persistence errors as well as their differences are greatest when the dynamic range of hemispheric ozone is largest. Therefore, one would expect the errors in the NH to be largest in the February-April period and smallest in the July-September period. However, even when the forecast error is at its largest (~21 DU), the percent of total column ozone is still quite small (21 DU (error) / 300 DU (normal ozone) = 7.0%).

# of Day Forecast	Regression RMS Error (DU)	Persistence RMS Error (DU)
2 Day	14.51	16.54
3 Day	17.59	19.56
4 Day	19.02	21.12
5 Day	21.86	22.65

Table 2. Mean RMS errors of Northern Hemisphere ozone forecasts and persistence of 2 to 5 days in length between December 24, 1993 and February 5, 1994.

In the event of missing satellite or forecast data, a decision tree (see Figure 3) has been developed. In the absence

been shown to work with the failure of the NOAA-11 SBUV/2 instrument in September 1994. The UVI was determined using the NOAA-11 TOVS from the failure of the NOAA-11 SBUV/2 until the NOAA-14 SBUV/2 became operational. At that time the program automatically switched to using the new ozone data. In the event of the MRF model run either failing or being late, the height and temperature fields from the previous model run, twelve hours earlier, are used to create the forecasts.

Computation of the Clear Sky UV Dose Rate at Sea Level

Once a forecast ozone field is available, the next step is to apply the radiative transfer model at each of the 1"x 1" grid points to determine the spectral irradiances at each wavelength between 290 and 400 nm. Other inputs include a parameterized value representing the atmospheric optical thickness, the UV albedo of the surface, the grid location's latitude, the day of year, and the solar time of day. The time of day is held constant(solar noon), as well as the UV albedo(5%), and the optical depth(0.2). The spectral irradiance values are weighted by a WMO-adopted standard action spectrum(McKinlay and Diffey, 1987). This action spectrum simulates the human skin's response to radiation at various wavelengths within the UV part of the spectrum. These weighted spectral irradiances are then integrated between 290 and 400 nm to produce an erythemal irradiance (mW/m^2) or dose rate for "clear sky" conditions at sea level. Running the radiative transfer model for each of the 181x360 grid points even on a CRAY-90 takes several minutes of CPU. An alternative time saving method of determining the dose rate value without significant loss of accuracy uses a three dimensional look up table with ozone, latitude and "day-of-year" as the inputs. The dose rate can vary globally from 0 to nearly 400 mW/m^2. A WMO-adapted standard of dividing this number by 25 m^2/mW results in the unitless UVI value. Doing so gives a global range of the UVI from 0 to nearly 16.

The EPA has developed five exposure categories of the UVI with appropriate actions for the public to protect themselves from overexposure to UV radiation. The categories, the UVI

Elevation Adjustments to the Sea Level Clear Sky Values

In order to make the dosage value realistic, the NWS reviewed which adjustments could be incorporated into the sea-surface "clear sky" value before the implementation of the 1994 Experimental UVI program. The most obvious and simplest modification to introduce is an adjustment due to elevation gain. As one rises above the sea level the thickness of the troposphere is lessened. Consequently, the amount of scattering also decreases, and incident UV radiation increases. The adjustment due to elevation has been studied by Frederick(personal communication), Blumthaler et al. (1992), and Blumthaler et al. (1994). Frederick cites an increase of 6% per km using model calculations while Blumthaler cites a larger 14-18% per km from direct observations. Our elevation adjustment, derived from Frederick's model, is of the form shown in Equation 4:

$$adj(\frac{\%}{km}) = a_0 + a_1 Z_{sfc} + a_2 Z_{sfc}^2 \quad (4)$$

where

a_0 = -0.04556,

a_1 = 6.62033,

a_2 = -0.23067

and Z_{sfc} is in kilometers.

The adjustment is a 6.34% increase for the first kilometer, and this rate decreases for each additional kilometer gained. The elevation adjustments are made at each grid point using the topography heights contained in the MRF model.

Determination of Adjustments Due to Cloud Probabilities

A simple method to introduce clouds into the UVI forecast is to correlate MOS cloud probabilities with the ratio of the measured UV amounts to the "clear sky" forecast. So that the wide variety of U.S. climatic conditions are represented, this calculation must use as many observation sites as possible within the U.S. We use 1992 data to develop the coefficients and 1993 data to independently test the results. Since data from a

sites with the most reliable data include: Albuquerque, NM, Concord, NH, Detroit, MI, El Paso, TX, Minneapolis, MN, Salt Lake City, UT, and Seattle, WA.

The forecasted MOS cloud probabilities for clear, scattered and broken clouds at these same cities are regressed against the ratio of the noontime "clear sky" dose rate and the 1992 RB observations. No coefficient is determined for overcast skies since its probability is algebraically dependent upon the other three probabilities (i.e. the sum of the probabilities equals one). The regression produced the following constant and clear, scattered and broken cloud coefficients with their respective 95% confidence limits:

Constant = 0.316 ± 0.172
Clear = 0.676 ± 0.037
Scattered = 0.580 ± 0.033
Broken = 0.410 ± 0.077.

Thus, under the probability of 100% clear sky the regression produces a cloud attenuation factor (CAF) of 0.992, under 100% scattered clouds: 0.896, under 100% broken: 0.726, and for 100% overcast: 0.316.

Skill

Verification: 1993

The 1993 RB data for the above cities are used as independent verification of the validity of the cloud regression coefficients. The correlation coefficient for CAFs from the MOS forecasts and the RB observations for 1993 is 0.668. The CAFs are used as one means of comparison as this removes the effect of the annual cycle imbedded in the data. A similar procedure using regressions with the MOS's "most likely" cloud category produces a correlation coefficient of only 0.576. When compared with RB observations the UVI is within one index unit 65% of the time and within two index units 89% of the time. Figures 4 shows the UVI forecasts and the RB observations at Detroit for the days of June 9 (day 160) through September 17 (day 270) of 1993. The

Verification: 1994

After the issuance of the Experimental UVI forecasts began in the summer of 1994, a number of additional verification sites became available from a collection of governmental agencies, cancer institutes and private firms. Table 4 displays the site location, operating agency or institute, the nearest surface city for which a UVI forecast could be made, and the type of instrument (broadband or spectral).

Figure 5 shows the 1-h average of observations about solar noon by a spectroradiometer operated by the EPA at Boston, MA with the UVI forecast and the "clear sky" forecast during the verification period of June 9 (day 160) through September 17 (day 270) 1994. Note again that the variability of the UVI is not as large as the actual observations. Most of the time the UVI forecast captures the essence of the observations. However, on cloudy days, the regression method results in UVI forecasts that are too high. This is a general tendecy that we attribute to several factors: 1. MOS rarely goes to 100% overcast/clear conditions, 2. we have no information on the radiative characteristics of these clouds and the statistics drive results toward the mean.

One additional feature is that using the UVI and solar noon hour observations may present a conservative estimate of the reliability of the UVI. Figure 6 shows a closer look at the Boston daily UV observations for July 9-19, 1994. This time, all of the 15 minute UV observations during the course of the day are plotted. Note that on some days that just before the peak time of solar insulation, clouds develop and cause a decrease in the UV observations. The peak times of these UV observations are not during the solar noon hour but before or after. The forecasted UVI seems to perform better against the peak observed UV observations as opposed to the 1-h average noontime values. This may be understandable since the MOS cloud probabilities are applicable for a 3-h period, not just the instant of solar noon.

Table 5 shows the resulting statistics for Boston and the 20

deviation of the CAFs shows how much more variable the observed cloud conditions are with respect to the forecasted cloud conditions. Correlation coefficients of the individual site's CAF_{OBS} and CAF_{UVI} range from a poor 0.242 at the NOAA's Albuquerque site to respectable 0.812 at USDA's Douglas Lake site. Note how the very clear sites have the highest mean CAF_{OBS}, low standard deviations and correlate the worst against the CAF_{UVI}, even though the mean difference between the forecasts and the observations is not very large. The mean and RMS of the (CAF_{UVI}-CAF_{OBS}) differences are better indicators of the correctness of the UVI forecast than correlation coefficient. Here we see that only 5 of the 21 sites have mean differences larger than ±1.0 index units. However, the RMS of the differences shows a range of variation between 1 and 2 index units. Figure 7 shows a histogram of the differences between the forecasted UVI and the noontime observations. The UVI forecasts are correct ($|diff| \leq 0.5$) 31.8% of the time, and are within 1 UVI unit ($|diff| \leq 1.5$) 75.9% of the time, and are within 2 UVI units ($|diff| \leq 2.5$) 91.5% of the time. This is consistent with the RMS differences discussed above.

Binning the forecasts and the observations into the EPA's exposure categories results in the values shown in Table 6. The computed "percent correct" value for this table is 60.7%. As Table 6 illustrates, the UVI tends to be conservative, occasionally overestimating on days with observations of "Minimal", "Low", or "Moderate", but rarely underestimating on days of "High" or "Very High" observations. It is important for the forecast to be correct when the observed UV falls in the "High" and "Very High" (H&VH) categories. For such cases correct H&VH forecasts (X) were made 517 times. H&VH observations but not forecasted (Y) occurred 105 times. H&VH forecasts (Z)but not observed occured 142 times. These numbers are used to compute the Probability of Detection (PoD) as illustrated in Equation 5:

$$PoD = \frac{X}{X + Y} \quad . \qquad (5)$$

Another statistic is the False Alarm Ratio (FAR). The FAR is the fraction of all H&VH event forecasts that were observed as "Moderate", "Low" or "Minimal" as illustrated in Equation 6:

$$FAR = \frac{Z}{X + Z} \quad . \qquad (6)$$

The more often an event is forecast, and does not occur the higher the score. A score of 0 indicates no false alarms. The H&VH values give a FAR of 0.215 indicating a low occurrence of false alarms.

In conclusion, the UVI forecasts tend to overestimate the UV radiation during cloudy days and underestimate it during clear days. This characteristic is in the nature of using a regression scheme to provide the CAF. However, the latter condition may be a result of the MOS forecasts rarely providing a 100% clear sky probability. In the opposite sense, the MOS forecasts will rarely forecast high non-clear probabilities when clear conditions actually are observed. This means that the UVI forecast will rarely be low when high values actually occur. Although the UVI forecast is verified during the noontime hour it has been shown that occasionally convective clouds form before noon and diminish the observed UVI. Within a few hours, these clouds dissipate and the observed UV are very close to that forecasted. However, taking the data as they are, the UVI forecasts are within one index unit nearly 76% of the time. For the most important conditions when the UVI values encompass the "High" and "Very High" exposure categories, the probability of detection is high, and the false alarm rate is low.

Summary

The National Weather Service makes use of existing observations and technology to derive a forecast of the potency of ultraviolet radiation at the surface during the peak hour with the inclusion of clouds. The means of forecasting the ozone

overestimate UV values under cloudy conditions and underestimate UV values in very clear conditions.

Description of the Bulletin

Figure 8 shows how the UVI forecasts are disseminated in the form of a bulletin. The AFOS identifier is "NMCUVICAC" and the WMO header is "AEUS41 KWBC". The bulletin uses the same city list used for the Selected Cities Weather Summary and Forecasts product. The UVI values are put into whole integers before dissemination. A preface gives information about the UVI, exposure categories as suggested by the EPA and Points of Contact for additional information are also included. The bulletin is generated about 18 UT following the completion of the 12Z MRF run.

Uses of Bulletin

As with other meteorological variables disseminated on selected city lists, the UVI bulletin gives information not only for the local station but for the entire country. This is useful year round information for travelers going from lower UVI locations to higher UVI locations. Forecast personnel should be made aware that the UVI applies for the immediate conditions (i.e. cloudiness and/or elevation) of the forecast office. Those weather offices in the mountain states should be aware of the changes in UVI due to elevation. Likewise, weather offices which include snowy areas or areas which include recreational waters and beaches should be aware of increased exposure to UV radiation due to reflection off of snow, water and light sand. One should be aware that if the forecast MOS cloud conditions for the 11am to 1pm LST are much different than observed, the forecast UVI most likely will reflect this difference. As mentioned earlier, the MOS cloud probabilities do not include Hawaii and Puerto Rico, and UVI forecasts in these locations use just the "clear sky" value.

References

American Cancer Society, Cancer Facts and Figures, 1994.

Blumthaler, M. and W. Ambach, Solar UV-B albedo of various surfaces, *Photochem. Photobiol.,48*, 85-88, 1988.

Blumthaler, M., W. Ambach, and W. Rehwald, Solar UV-A and UV-B Radiation fluxes at two alpine stations at different altitudes, *Theor. Appl. Climatol., 46*, 39-44, 1992.

Blumthaler, M., A.R. Webb, G. Seckmeyer, A.F. Bais, M. Huber and B. Mayer, Simultaneous spectroradiometry: a study of solar UV irradiance at two altitudes, *Geophys. Res. Lett., 21,* 2805-2808, 1994.

Colmar Brunton Research, National Ominibus Telephone Survey of 1000 People, Cancer Society of New Zealand, Wellington, NZ, 1992.

Coulson, K.L. and D.W. Reynolds, The spectral reflectance of natural surfaces, *J. Appl. Meterol, 10*, 1285-1295, 1971.

Decima Research, An investigation of Canadian's attitudes related to Environment Canada's UV index, 6pp, available at authors request, 1993.

DeFabo, E.C. and F.P. Noonan, Mechanism of immune suppression by ultraviolet radiation in vivo.I. Evidence for the existence of a unique photoreceptor in skin and its role in photoimmunology, *J. Exp. Med., 158*, 84-98, 1983.

Frederick, J.E. and D. Lubin, The budget of biologically active radiation in the earth-atmosphere system, *J. Geoph. Res., 93*, 3825-3832, 1988.

Hill, D., V. White, R. Marks and R. Borland, Primary prevention of melanoma. A longitudinal study of sunburn reduction in an

ultraviolet induced erythema in human skin, *Human Exposure to Ultraviolet Radiation: Risks and Regulations*, W.F. Passchier and B.F. Bosnajakovic, Eds, pp 83-87, Elsevier, Amsterdam, 1987.

Miller, A.J., R.M. Nagatani, J.D. Laver and B. Korty, Utilization of 100 mb mid-latitude height fields as an indicator of sampling effects of total ozone variations, *Mo. Wea. Rev., 107*, 782-787, 1979.

Nagatani, R.M., J.D. Laver and A.J. Miller, Backscatter ultraviolet (BUV) ozone analysis system, NWS/NMC Office Note 132, 15pp, March 1977.

Wilson, L.J., Canada's UV index - how it is computed and disseminated, Environment Canada, Atmospheric Environment Service, Downsview, Ontario, Canada, 1993.

Figures

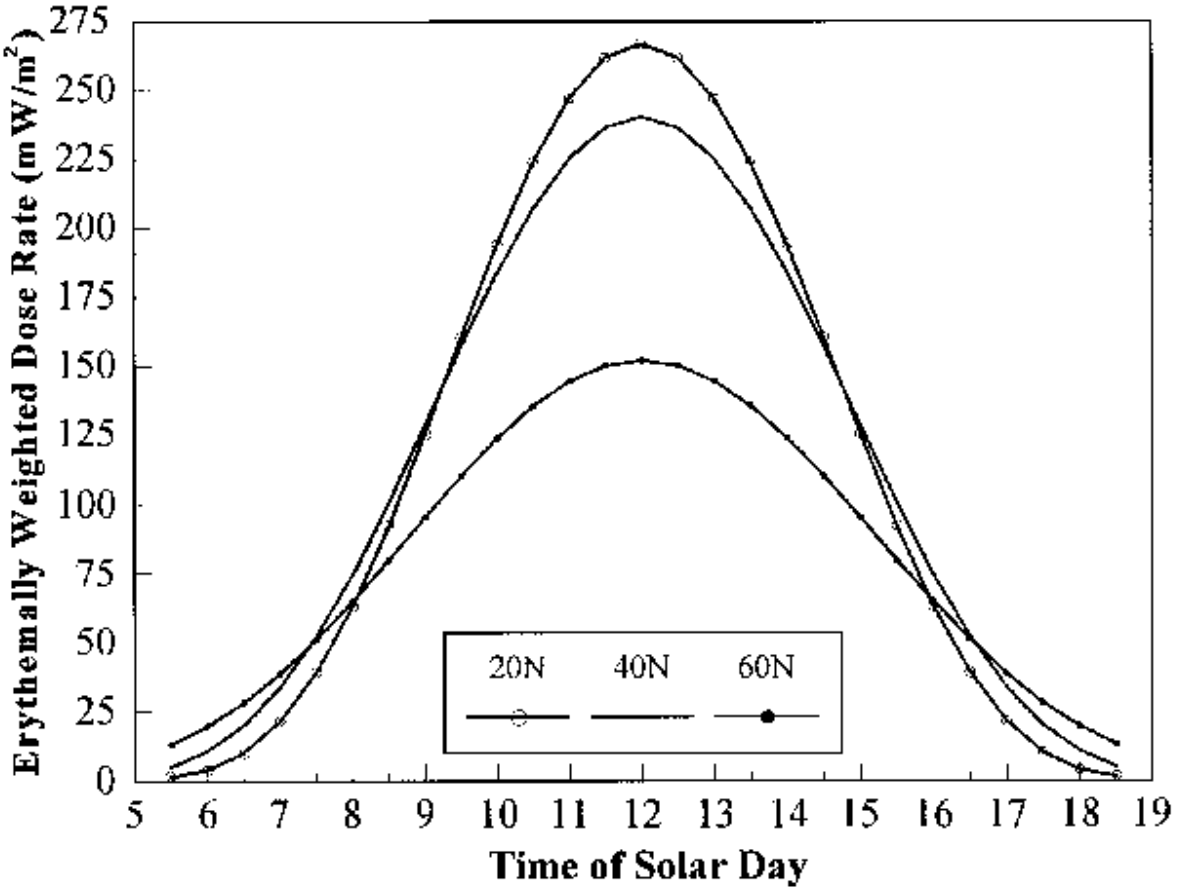

Figure 1. Diurnal curves of erythemal dose rates(mW/m^2) at 20°N, 40°N, and 60°N at summer solstice with 300 DU of ozone overhead. Note that as higher latitudes are approached, the diurnal curve during the solar noon hour flattens.

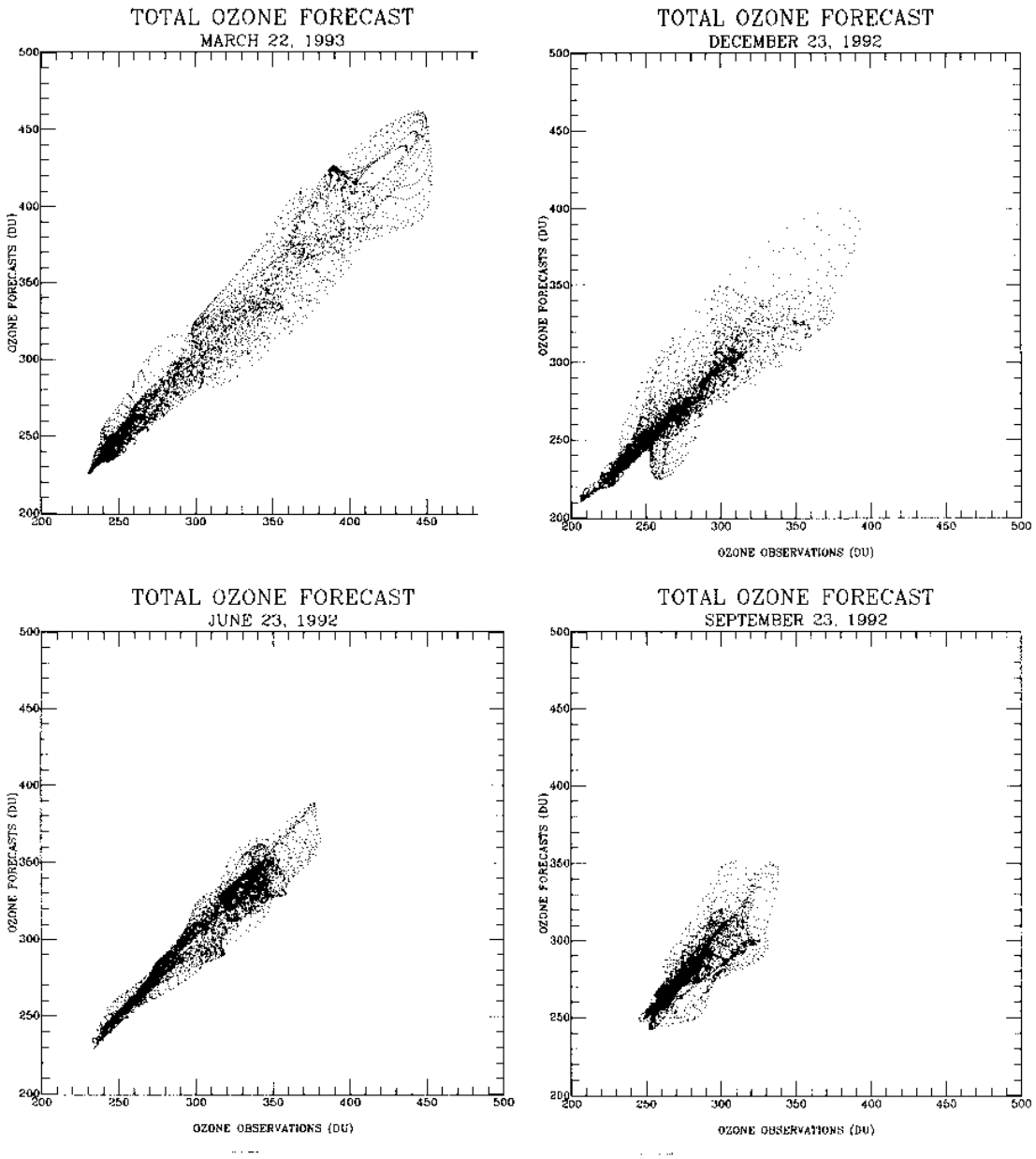

Figure 2. Comparison of Northern Hemisphere total ozone forecasts versus that observed by the SBUV/2 instrument on board NOAA-11 for: a) March 22, 1993; b) June 23, 1992; c) September 23, 1992; and d) December 23, 1992. Note how the dynamic range is greatest in March and smallest in September.

UV INDEX DECISION TREE:

- Get [D-1] Ozone (SBUV/2 & TOVS) Files from Front End Computer
- Get D, D+1 Z_{500}, Z_{100} and T_{50} MRF Fields
- Get [D-2] Ozone Files
- Get [D-1] & [D-2] Z_{500}, Z_{100} and T_{50} Files
- Convert from Polar to Lat/Lon Fields
- Determine Differences ([D-1] - [D-2]) for O_3, Z AND T Fields
- Determine Regression between O_3 and Z, T Fields for NH & SH
- Determine Differences ([D+1] - [D-1]) for Z and T Fields
- Use Regressions to Determine ([D+1] - [D-1]) Differences for O_3
- Add O_3 Differences to [D-1] Field to get [D+1] O_3 Field
- Use Radiative Transfer LUT to get "CLEAR SKY" Sea Level Dose Rates
- Determine Hourly Dosage Adjusted for Elevation at MOS Cities
- Create Bulletin for Dissemination

OZONE DATA ACCESSING DECISIONS:

- IF SBUV/2 Ozone Field is Not Available for [D-1],
  THEN the Regression Coefficients for the Last Available Preceding Day is Used
  (Up to 4 Days) to Create the Ozone Forecast.

- IF the Most Recent SBUV/2 Data is Older than 4 Days,
  THEN the Most Recent TOVS Ozone Data is Used.

- IF the Most Recent TOVS Data is Older than 4 Days,
  THEN IF there is a SBUV/2 Ozone Field Available in the Last 4 Days,
  THEN it is Used Assuming Persistence.

- IF there is No SBUV/2 Field in the Last 4 Days,
  THEN IF there is a TOVS Ozone Field Available in the Last 4 Days,
  THEN it is Used Assuming Persistence.

- IF there is Neither a SBUV/2 or TOVS Ozone Field in the Last 4 Days,
  THEN the Program Ends.

Figure 3. Decision tree of UV Index processing and data accessing made prior to each run of the UV Index. D is the current day, [D-1] is yesterday, [D-2] is 2 days ago, and [D+1] is tomorrow.

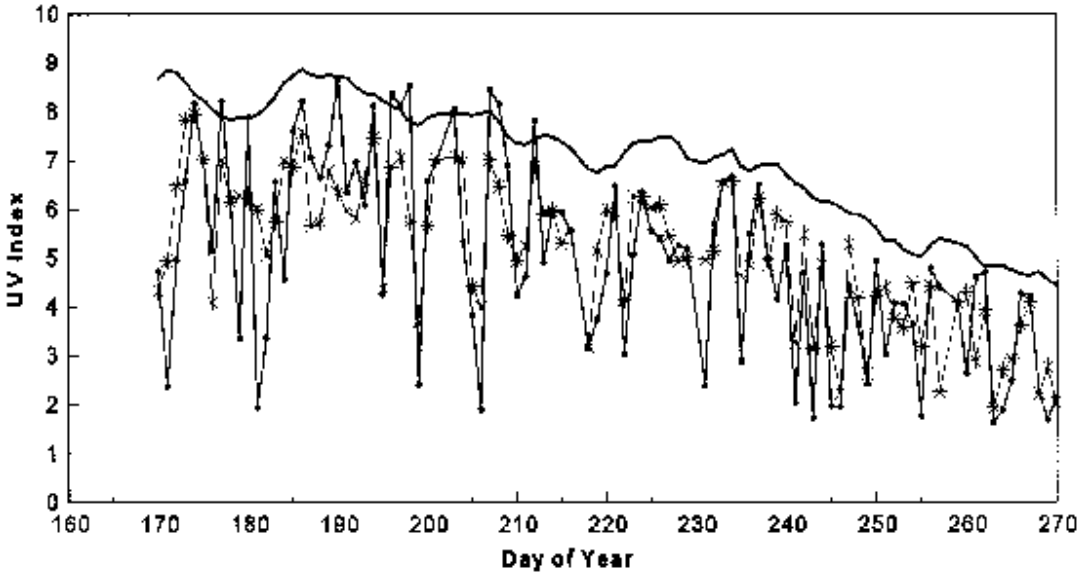

Figure 4. Daily RB noontime UV observations (solid line with closed circle), UVI forecast from regression coefficients (solid line with star), and "clear sky" UVI (bold solid line) for the period of days 160-270 (June 9 to September 17), 1993 at Detroit, MI.

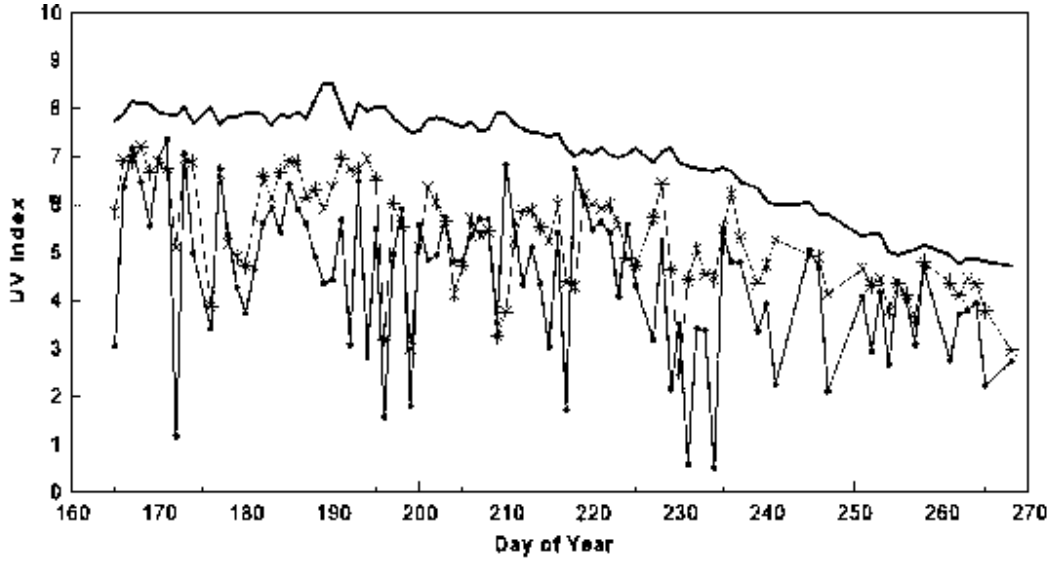

Figure 5. Daily noontime spectroradiometer UV observations (solid line with colosd circle), UVI forecast (solid line with starr), and "clear sky" UVI (bold solid line) for the period of days 160-270 (June9 to September 17), 1994 at Boston, MA.

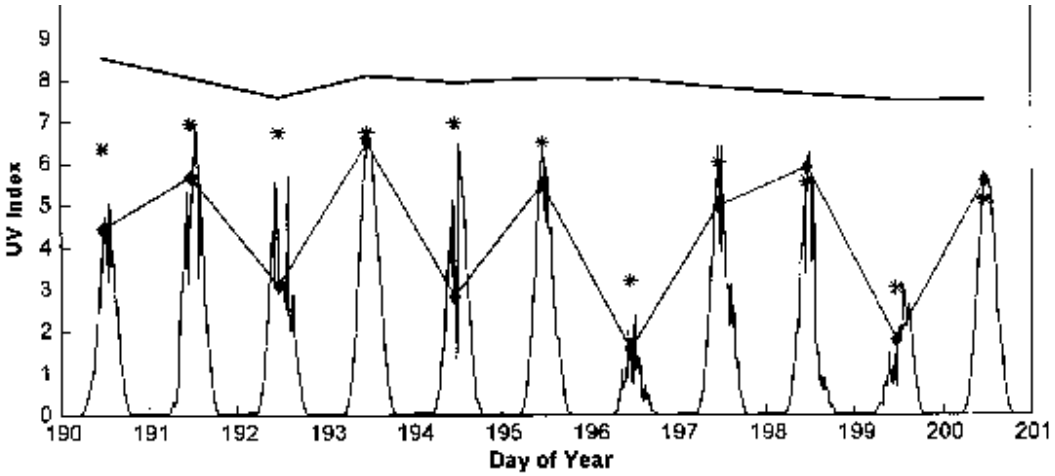

Figure 6. Diurnal spectroradiometer UV observations (solid line), noontime observations (lines with diamonds) UVI forecasts (asterisks), and "clear sky" UVI (thick solid line) for Boston, MA for days 190-200 (July 9-19), 1994.

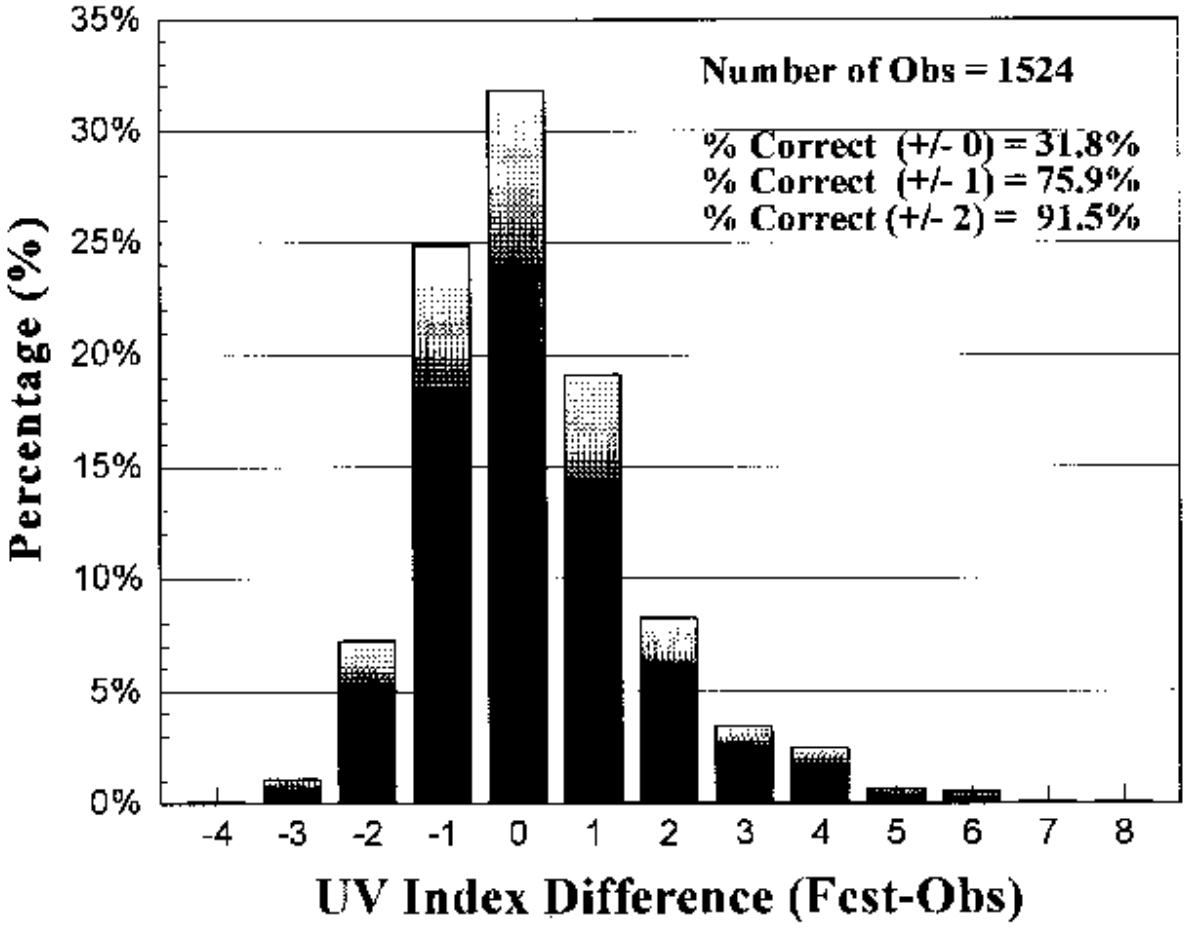

Figure 7. Histogram of the (UVI Forecast - UV observation) differences in whole UVI units for all 21 sites between July and October, 1994.

AEUS41 KBWC NMCUVICAC

NOAA/EPA ULTRAVIOLET INDEX /UVI/ FORECAST
CLIMATE ANALYSIS CENTER NMC
NATIONAL WEATHER SERVICE WASHINGTON DC
159 PM EDT MON JUL 1 1996

VALID JUL 2 1996 AT SOLAR NOON /APPROXIMATELY NOON
LOCAL STANDARD TIME OR 100 PM LOCAL DAYLIGHT TIME

THE UV INDEX IS CATEGORIZED BY EPA AS FOLLOWS

UVI	EXPOSURE LEVEL
0 1 2	MINIMAL
3 4	LOW
5 6	MODERATE
7 8 9	HIGH
10 AND GREATER	VERY HIGH

FOR HEALTH RELATED ISSUES...CONTACT EPA AT 1-800-296-1996 OR CDC 404-488-4347. FOR TECHNICAL INFORMATION ON HOW UVI VALUES ARE GENERATED...CONTACT THE NATIONAL WEATHER SERVICE AT 301-713-0622.

CITY	STATE	UVI	CITY	STATE	UVI
ALBUQUERQUE	NM	10	LITTLE ROCK	AR	8
ANCHORAGE	AK	4	LOS ANGELES	CA	10
ATLANTA	GA	10	LOUISVILLE	KY	7
ATLANTIC CITY	NJ	6	MEMPHIS	TN	8
BALTIMORE	MD	6	MIAMI	FL	9
BILLINGS	MT	8	MILWAUKEE	WI	6
BISMARCK	ND	8	MINNEAPOLIS	MN	8
BOISE	ID	8	MOBILE	AL	10
BOSTON	MA	7	NEW ORLEANS	LA	9
BUFFALO	NY	6	NEW YORK	NY	6
BURLINGTON	VT	7	NORFOLK	VA	7
CHARLESTON	SC	10	OKLAHOMA CITY	OK	9
CHARLESTON	WV	7	OMAHA	NE	9
CHEYENNE	WY	10	PHILADELPHIA	PA	6
CHICAGO	IL	7	PHOENIX	AZ	10
CLEVELAND	OH	6	PITTSBURGH	PA	6
CONCORD	NH	7	PORTLAND	ME	7
DALLAS	TX	9	PORTLAND	OR	6
DENVER	CO	10	PROVIDENCE	RI	7
DES MOINES	IA	9	RALEIGH	NC	8
DETROIT	MI	5	SALT LAKE CITY	UT	10
DOVER	DE	6	SAN FRANCISCO	CA	10
HARTFORD	CT	7	SAN JUAN	PU	11
HONOLULU	HI	11	SEATTLE	WA	6
HOUSTON	TX	9	SIOUX FALLS	SD	9
INDIANAPOLIS	IN	7	ST. LOUIS	MO	8
JACKSON	MS	9	TAMPA	FL	9
JACKSONVILLE	FL	10	WASHINGTON	DC	6
LAS VEGAS	NV	10	WICHITA	KS	9

Figure 8. UVI bulletin as sent through AFOS.